scientific reports

Check for updates

OPEN

Metformin hydrochloride improves hepatic glucolipid metabolism in diabetes progression through SIRT5-mediated ECHA desuccinylation

Liang Tang[1], Qing Sun[2], Jinling Luo[3] & Suying Peng[4]✉

The management of hyperglycemia and lipid metabolism is pivotal for the treatment of type 2 diabetes mellitus (T2DM). Metformin hydrochloride (DMBG) remains the most widely prescribed medication for this condition. This study aimed to elucidate the effects and underlying mechanisms by which DMBG enhances glucolipid metabolism using both in vivo and in vitro experimental models. Animal models were established using high-fat diet (HFD)-fed mice, while cellular models utilized palmitic acid (PA)-induced HepG2 cells. In vivo, the impact of DMBG on glucolipid metabolism was evaluated through measurements of insulin and HbA1c levels, intraperitoneal glucose tolerance tests (ipGTT), intraperitoneal insulin tolerance tests (ipITT), as well as histological assessments with hematoxylin-eosin (HE) and Oil-red O staining. Mitochondrial function was assessed via biochemical assays of TBARS, SOD, ATP, and H2O2 levels in liver tissue, alongside determinations of mitochondrial membrane potential, ROS production, mtDNA content, and SIRT5 mRNA expression. For in vitro analysis, glucose consumption, mitochondrial membrane potential, ROS levels, and protein expressions of AMPK and PGC-1α were quantified in HepG2 cells. Western blotting and co-immunoprecipitation (co-IP) techniques were employed to investigate the mechanistic pathways involved. Treatment with DMBG resulted in reduced levels of free fatty acids, body weight, and fat mass, while also alleviating hyperglycemia and hepatic lipid accumulation in HFD-fed mice. Furthermore, DMBG restored impaired mitochondrial function in these animals and increased SIRT5 expression via AMPK activation. In vitro, DMBG mitigated PA-induced alterations in glucose consumption and mitochondrial dysfunction in HepG2 cells, an effect that was abrogated upon SIRT5 knockdown. Overexpression of SIRT5 led to enhanced trifunctional enzyme subunit-alpha (ECHA) desuccinylation at the K540 site, thereby increasing its activity. Collectively, our findings indicate that DMBG improves hepatic glucolipid metabolism through a mechanism involving SIRT5-mediated ECHA desuccinylation, potentially offering a new therapeutic avenue for T2DM.

Keywords Metformin hydrochloride, Hyperglycemia, Lipid metabolism, Desuccinylation, ECHA

Type 2 diabetes mellitus (T2DM), also known as non-insulin-dependent diabetes mellitus, represents a significant health challenge of the 21st century. Characterized by chronic hyperglycemia and insulin resistance (IR), T2DM is a multifactorial disease with complex etiology[1]. Despite ongoing research, the precise mechanisms underlying its pathogenesis remain to be fully elucidated. However, evidence supports that prolonged consumption of a high-fat diet (HFD) plays a pivotal role in precipitating systemic abnormalities in glucose tolerance and IR, which are closely associated with increased mitochondrial dysfunction[2–4]. The liver, an organ central to maintaining glucose and lipid homeostasis, is particularly vulnerable to HFD-induced alterations. Studies

[1]Comprehensive Internal Medicine Department of High tech Industrial Park, Chongqing University Fuling Hospital, No. 32 Juye Avenue, High tech Zone, Fuling District, Chongqing 408000, China. [2]Medical Clinical Nutrition Department, Chongqing Uniersity Fuling Hospital, No. 2 Gaosuntang Road, Fuling District, Chongqing 408000, China. [3]Medical Laboratory, Chongqing University Fuling Hospital, No. 2 Gaosuntang Road, Fuling District, Chongqing 408000, China. [4]Nephrology Department, Chongqing University Fuling Hospital, No. 2 Gaosuntang Road, Fuling District, Chongqing 408000, China. ✉email: pengsuying@cqu.edu.cn

have demonstrated that HFD can lead to hepatic steatosis and exacerbate IR, contributing significantly to the development of T2DM[4,5]. Moreover, T2DM is linked to mitochondrial damage, wherein elevated glucose levels promote excessive production of mitochondrial reactive oxygen species (ROS). This overproduction triggers oxidative stress and lipid peroxidation, further deteriorating cellular function[6]. Given these considerations, strategies aimed at controlling hyperglycemia and correcting aberrant lipid metabolism present promising avenues for mitigating the progression and complications of T2DM. Addressing mitochondrial dysfunction may also prove crucial in developing effective therapeutic interventions.

Metformin hydrochloride (DMBG) stands as the first-line therapeutic agent for T2DM, favored for its affordability and favorable safety profile. DMBG exhibits robust hypoglycemic efficacy by suppressing hepatic gluconeogenesis and glycogenolysis, which contributes to improved glucose homeostasis[7,8]. Beyond its primary application in diabetes management, DMBG has demonstrated beneficial effects in a broad spectrum of conditions, including cardiovascular disease, renal disorders, oncological indications, and neurodegenerative diseases[9–12]. Despite the extensive clinical utility of DMBG and its established role in activating AMP-activated protein kinase (AMPK), which underlies many of its metabolic benefits, the full repertoire of molecular targets remains incompletely characterized. This gap in knowledge restricts a comprehensive understanding of DMBG's mechanisms of action and potentially limits its therapeutic optimization. Further elucidation of these molecular pathways is essential to fully harness the therapeutic potential of DMBG across diverse medical applications.

Lysine succinylation is a post-translational modification wherein a succinyl group is covalently attached to the ε-amino group of a lysine residue within a substrate protein, occurring through either enzymatic or non-enzymatic mechanisms. The extent of succinylation is regulated by the availability of succinyl donors and the activity of specific enzymes, including succinyltransferases and desuccinylases[13]. Sirtuin 5 (SIRT5), a conserved NAD+-dependent desuccinylase predominantly localized in mitochondria, plays a critical role in cellular metabolism[14]. Emerging evidence indicates that SIRT5 functions as an essential sensor of cellular energy status and provides protection against metabolic stress[15,16]. Additionally, SIRT5 has been shown to mitigate oxidative stress and enhance mitochondrial function, thereby ameliorating IR in insulin-sensitive tissues such as skeletal muscle and adipose tissue[17]. Furthermore, studies have reported that DMBG can upregulate SIRT5 expression via AMPK activation, leading to improvements in hyperglycemia and lipid metabolism[18]. However, the extent to which DMBG modulates succinylation through SIRT5 in the context of T2DM remains an open question warranting further investigation.

Trifunctional enzyme subunit-alpha (ECHA), also known as HADHA or MTPα, is a critical component of the mitochondrial β-oxidation pathway, catalyzing the final three steps in the oxidation of long-chain fatty acids. Recent studies have highlighted the role of ECHA in regulating hepatic glucose and lipid metabolism. Overexpression of ECHA has been shown to inhibit hepatic glucose production in mice, whereas its knockdown enhances the glucagon response[19]. Additionally, increased expression of ECHA has been associated with reduced oxidative stress and alleviation of hepatic steatosis in models of non-alcoholic fatty liver disease (NAFLD)[20]. Given these findings, ECHA emerges as a potential therapeutic target for addressing hyperglycemia and abnormal lipid metabolism in T2DM. Its modulation may offer a novel strategy to correct metabolic dysregulation associated with this condition.

In this study, we systematically investigated the effects and underlying mechanisms by which DMBG ameliorates hyperglycemia and abnormal lipid metabolism in both in vivo and in vitro models. This investigation not only contributes to the existing body of knowledge regarding DMBG's mechanisms of action but also may uncover innovative therapeutic strategies for managing T2DM and its associated complications.

Methods

Animal study

The study was approved by the Ethics Committee of MDKN Biotechnology Co., Lt. All experiments were performed in accordance with relevant guidelines and regulations. This study is reported in accordance with ARRIVE guidelines.

C57BL/6 mice were obtained from Charles River Laboratories (Beijing, China). Upon arrival, the animals were acclimatized for two weeks in a controlled environment maintained at 22 ± 2 °C with a 12-hour light/12-hour dark cycle. Throughout this period, mice had ad libitum access to standard chow and water. The mice were randomly allocated into three groups ($n = 6$ per group): a normal diet group (ND), a high-fat diet group (HFD), and a high-fat diet plus metformin hydrochloride group (HFD + DMBG). Mice in the HFD and HFD + DMBG groups were fed a high-fat diet (HFD) composed of 42% fat, 28% protein, and less than 1% carbohydrate for 6 weeks. The ND group was maintained on a standard chow diet throughout the study period. To standardize food intake, mice in each group were provided with 4 g of their respective diets daily. To establish a T2DM mouse model, mice fed the HFD received intraperitoneal injections of streptozotocin (STZ) at a dose of 50 mg/kg body weight. The initial injection was administered on the first day following the completion of the 6-week HFD regimen. Subsequent injections were performed every other day for a total of six administrations. Mice in the ND group were injected intraperitoneally with an equivalent volume of saline, following the same protocol as for the STZ injections. Subsequently, mice in the HFD + DMBG group received DMBG at a dose of 150 mg/kg via gavage daily for 8 weeks, while mice in the ND and HFD groups received physiological saline by gavage using the same regimen. During this treatment period, all mice were provided with a ND. After the 8-week DMBG treatment, body weight was recorded, and fat mass was measured using a body composition analyzer (Bruker, Billerica, MA, USA). Blood samples were collected from the tail vein and centrifuged to isolate serum. At the conclusion of the experiment, mice were euthanized via intraperitoneal injection of pentobarbital sodium (160 mg/kg), and livers were excised for further analysis.

Hematoxylin Eosin (HE) staining and oil red O staining

To evaluate the pathological changes and lipid accumulation in the livers of mice, Hematoxylin Eosin (HE) staining and Oil Red O staining were performed using commercially available kits (Beyotime, Beijing, China). Liver tissues were harvested and immediately fixed in 10% neutral-buffered paraformaldehyde for 24 h. Following fixation, tissues were processed for paraffin embedding. Paraffin-embedded liver Sect. (5 μm thick) were prepared and subjected to HE staining or Oil Red O staining according to the manufacturer's protocols. For HE staining, sections were deparaffinized and rehydrated through a series of graded alcohols and xylene substitutes, stained with hematoxylin for nuclear visualization, differentiated, and counterstained with eosin to highlight cytoplasmic components. For Oil Red O staining, sections were similarly deparaffinized and rehydrated, then incubated with Oil Red O working solution to stain lipid droplets, followed by counterstaining with hematoxylin. Stained sections were examined under a light microscope, and representative images were captured for further analysis. The extent of hepatic steatosis was assessed qualitatively and quantitatively as appropriate.

Cell culture and treatment

HepG2 cells, obtained from the ATCC (Manassas, VA, USA), were maintained in Dulbecco's modified eagle's medium (DMEM; Gibco, Thermo Scientific, Grand Island, NY, USA) supplemented with 10% fetal bovine serum (FBS; Gibco) and 1% penicillin-streptomycin. Cells were cultured in a humidified incubator at 37 °C with 5% CO_2. To mimic the diabetic environment, HepG2 cells were treated with 1 mM palmitic acid (PA; MedChemExpress, Monmouth Junction, NJ, USA) for 24 h. PA was dissolved in ethanol and conjugated to fatty acid-free bovine serum albumin (BSA) at a molar ratio of 5:1 (PA: BSA) before use. To evaluate the effect of DMBG on mitochondrial function in PA-induced HepG2 cells, cells were pre-treated with 2 mM DMBG (Merck, Darmstadt, Germany) for 24 h prior to and during PA exposure.

Cell transfection

For transfection experiments, HepG2 cells were seeded into 6-well plates at a density of 3×10^5 cells per well and allowed to adhere overnight. SIRT5 overexpressing plasmids and the empty vector (pcDNA3.1) were obtained from GenePharma (Shanghai, China). Transfections were performed using Lipofectamine 2000 (Invitrogen, Carlsbad, CA, USA) according to the manufacturer's protocol. Cells were incubated with the transfection complexes for 48 h to ensure adequate expression of the transfected constructs.

Free fatty acid (FFA) content detection

The levels of FFAs were measured by gas chromatography-mass spectrometry (GC-MS). The blood was centrifuged at 1000×g for 10 min to collect serum. The serum of mice (200 μL) in the different groups was placed in a 10 mL glass test tube. Then, 5 μL of BHT (4 μg/μL), 50 μL of 0.05% H_2SO_4, and 1 mL of a mixture of ethyl acetate/toluene (V: V = 2:1) were added to the tube. Next, the tube vortexed for 1 min and centrifuged for 10 min at 1000×g. The supernatant was transferred to a new glass test tube, and 50 μL of 0.05% H_2SO_4 and 1 mL of a mixture of ethyl acetate/toluene (V: V = 2:1) were added to the underlayer solution for 10 min centrifugation at 1000×g to collect supernatant. The two supernatants were mixed and blown dry with nitrogen at 40℃. After the supernatants were blown dry, 2 mL of 5% H_2SO_4/CH_3OH and 0.5 mL of toluene were and mixed well, and then transferred to a headspace flask and placed in a 70℃ water bath for 70 min derivatisation. After the samples were cooled to room temperature, 2 mL n-hexane and 1 mL saturated sodium chloride were added and centrifuged for 10 min at 1000×g, and the supernatant was dried with nitrogen at 40℃. The samples were reconstituted with 400 μL of hexane, shaken for 1 min, filtered through 0.22 μm organic filter membrane and then measured. The free fatty acid content was obtained by checking the standard curve with the peak area.

Enzyme-linked immunosorbent assay (ELISA)

Mouse insulin ELISA kit (Sangon, Shanghai, China) and mouse hemoglobin A1c (HbA1c) ELSA kit (Abcam, Cambridge, UK) were utilized to measure the levels of insulin and HbA1c in serums of mice. The experiments were performed according to the manufacturer's protocol.

Intraperitoneal glucose tolerance test (ip GTT) and intraperitoneal insulin tolerance test (ip ITT)

The experiments of ip GTT and ip ITT was performed after the treatment of DMBG. For ip GTT, mice were received an intraperitoneal injection of glucose (2 g/kg) after fasting for 12 h. For ip ITT, mice were fasten for 8 h and then given an intraperitoneal injection of insulin (0.75 U/kg). The blood glucose was measured using a glucometer (Roche, Mannheim, Germany) after injection of 0, 15, 30, 60, 90 and 120 min.

Biochemical assays

The levels of thiobarbituric acid reactive substances (TBARS), superoxide dismutase (SOD), adenosine triphosphate (ATP) and H_2O_2 in liver tissues of mice, as well as glucose consumption of HepG2 cells were detected using a TBARS colorimetric assay kit (Elabscience, Wuhan, China), a SOD assay kit (Beyotime), an ATP assay kit (Beyotime), a H_2O_2 assay kit (Beyotime) and a glucose assay kit (Beyotime), respectively. The experiments were performed according to the manufacturer's protocol.

Isolation of mitochondria in liver tissues

The hepatic mitochondria was isolated using a mitochondrial isolation kit (Solarbio, Beijing, China). Tissues from mice livers were washed with phosphate-buffered saline (PBS) and homogenized with pre-cooled lysis buffer. Then, homogenized liver tissues were centrifuged at 1000×g for 5 min at 4℃ to collect supernatants.

Next, the supernatants were centrifuged at 12,000×g for 10 min at 4℃, and the mitochondria precipitates were at the bottom of the tube. The mitochondrial precipitates were suspended in 0.5 mL wash buffer and centrifuged at 1000×g at 4℃ for 5 min to collect supernatants. The supernatants were centrifuged at 12,000×g for 10 min at 4℃. Then, the supernatants were discarded and the mitochondrial precipitates were resuspended in 50 μl store buffer.

Measurement of mitochondrial membrane potential

The mitochondrial membrane potential was evaluated using a mitochondrial membrane potential assay kit with JC-1 (Beyotime). For isolated mitochondria, 10 μg mitochondria was stained with 0.9 ml JC-1 staining solution. For HepG2 cells, cells were incubated with 0.5 ml JC-1 staining solution for 20 min at 37℃ and then centrifuged at 600×g for 3 min at 4℃ to precipitate cells. Next, cells were resuspended in JC-1 staining solution for the subsequent detection. The excitation and emission wavelengths of JC-1 monomer are 490 nm and 530 nm, respectively, and the excitation and emission wavelengths of JC-1 polymer are 525 nm and 590 nm, respectively. The fluorescence intensity is expressed as polymer/monomer.

Measurement of mitochondrial ROS

The mitochondrial ROS intensity was assessed using an ROS assay kit (Beyotime). Isolated mitochondria and HepG2 cells were incubated with 10 μM DCFH-DA for 20 min at 37℃. The mitochondrial and cells were observed using a laser scanning confocal microscope. The excitation and emission wavelengths of DCFH-DA were 488 nm and 525 nm, respectively.

Measurement of mitochondrial DNA (mtDNA)

The mtDNA was isolated using a mtDNA isolation kit (Abcam). The levels of mtDNA in mice were evaluated through quantitative real-time PCR (qPCR) using an mouse mtDNA copy number kit (AmyJet Scientific, Wuhan, China) and a human mtDNA monitoring primer set (Takara, Tokyo, Japan), respectively.

qPCR

Total RNA of mice serums and HepG2 cells was isolated using Trizol reagent (Thermo Scientific). Next, a 1st Strand cDNA synthesis kit (Yeasen, Shanghai, China) was performed to reverse transcribe RNA into cDNA. qPCR was performed using SYBR green mix (Vazyme, Nanjing, China) on an Applied Biosystems (Thermo Scientific). Relative mRNA expression was calculated using the $2^{-\Delta\Delta Ct}$ method as normalized to GAPDH. The qPCR primers of SIRT5 are as follows: mouse, 5'-CCAGTTGTGTTGTAGACGAAAGC-3' (sense) and 5'-TTCC GAAAGTCTGCCATATTTGA-3' (antisense); human, 5'-GCCATAGCCGAGTGTGAGAC-3' (sense) and 5'-C AACTCCACAAGAGGTACATCG-3' (antisense).

Western blot

Cells were lysed using radioimmunoprecipitation assay (RIPA) lysis buffer and quantified using a bicinchoninic acid (BCA) kit (Vazyme). Next, the protein samples were loaded on sodium dodecyl sulfate polyacrylamide gel electrophoresis. After electrophoretic separation, the protein samples were transferred to polyvinylidene fluoride membranes. The membranes were blocked with 5% defatted milk for 1 h at room temperature and incubated with primary antibodies overnight at 4℃. Then, the membranes were blocked with secondary antibodies (1: 10000, ab205718, Abcam, Cambridge, UK) for 2 h, and the images were captured with enhanced chemiluminescence reagent (Beyotime). The band signals were visualized by Image J software. The primary antibodies including anti-p-AMPK (ab133448, 1: 1000, Abcam), anti-AMPK (ab32047, 1: 1000, Abcam), anti-PGC-1α (ab133448, 1: 1000, Abcam), anti-SIRT5 (ab259967, 1: 1000, Abcam), anti-ECHA (ab203114, 1: 1000, Abcam), anti-succinyllysine (1: 2000, PTM-401, PTM BIO, Hangzhou, China) and anti-GAPDH (ab181602, 1: 10000, Abcam).

Co-immunoprecipitation (co-IP) and IP

Co-IP was performed to assess the interaction between SIRT5 and ECAH, and the ECHA succinylation level was assessed by IP before western blot. Pierce classic magnetic IP/co-IP kit (Thermo Scientific) was used for the experiments. Briefly, cells were lysed for 5 min on ice with a dedicated lysis buffer. Then, the lysate was centrifuged at 13,000×g for 10 min and to collect supernatant and incubated overnight with antibodies (anti-Flag, anti-HA, anti-IgG or anti-ECHA) at 4 °C. Next, the mixture was incubated with Protein A/G magnetic beads at room temperature for 1 h. Finally, the beads were collected. The antigen-antibody mixture was eluted. The levels of proteins were measured by western blot.

Bioinformatic analysis

The succinylation sites of ECHA were predicted using the GPSuc database (http://kurata14.bio.kyutech.ac.jp/GPSuc/index.php).

ECHA stability detection

For assessment of protein stability of ECHA, cells were treated with 10 μM cycloheximide (MKBio, Shanghai, China) and the protein levels were measured after 0, 6, 12 and 24 h of treatment.

Statistical analysis

All data were analyzed using GraphPad Prism V.8.2.0. Results were expressed as mean ± standard deviation of at least three replicates. Comparison between two groups was determined by Student's t-test. The significant

differences in more than two experimental groups were compared with one-way ANOVA. $P<0.05$ was considered statistically significant.

Results

DMBG inhibits the content of FFAs and hepatic lipid accumulation in HFD mice

To elucidate the impact of DMBG on lipid metabolism, we evaluated its effects on FFA levels. As illustrated in Fig. 1A, HFD significantly elevated the levels of C16:0, C16:1, C18:1, and C18:2 FFAs, particularly for C16:1, C18:1, and C18:2. Notably, the levels of C18:0 and C22:4 were not affected by HFD. Importantly, treatment with DMBG markedly reversed the HFD-induced increases in all aforementioned FFA species (Fig. 1A). Histopathological examination of liver tissues via H&E staining revealed that HFD exacerbated pathological alterations in liver tissue structure, characterized by increased steatosis and inflammatory cell infiltration (Fig. 2H). These pathological changes were significantly ameliorated by DMBG treatment. Furthermore, Oil Red O staining demonstrated a pronounced increase in hepatic lipid droplets in HFD-fed mice, which was notably attenuated following DMBG administration (Fig. 2H and I). Collectively, these findings indicate that DMBG effectively suppresses FFA levels and mitigates hepatic lipid accumulation in HFD-fed mice.

DMBG improves hyperglycemia in HFD mice

To evaluate the effect of DMBG on hyperglycemia in vivo, we conducted a series of metabolic assessments. Results suggested that DMBG improved the survival rate of HFD mice (Fig. 2A). Moreover, HFD significantly increased body weight, fat mass, and insulin levels in mice, as shown in Fig. 2B and C, and 2D, respectively. Notably, these parameters were partially restored by DMBG treatment, suggesting an improvement in overall metabolic health. ipGTT revealed that blood glucose levels were markedly elevated in HFD-fed mice 30 min post-glucose administration, indicating impaired glucose clearance (Fig. 2E). Treatment with DMBG effectively reversed this trend, demonstrating improved glucose tolerance. Furthermore, ipITT showed that HFD-fed mice exhibited significantly higher blood glucose levels compared to control animals, indicative of insulin resistance (Fig. 2F). DMBG administration partially mitigated this effect, suggesting enhanced insulin sensitivity. Additionally, we measured HbA1c levels. As depicted in Fig. 2G, HFD led to a significant increase in HbA1c levels, which was normalized by DMBG treatment. Collectively, these findings demonstrate that DMBG effectively ameliorated hyperglycemia in HFD-fed mice, likely through mechanisms involving the restoration of glucose homeostasis and enhancement of insulin sensitivity.

DMBG alleviates the mitochondrial dysfunction in HFD mice

To investigate the effects of DMBG on mitochondrial function in HFD-fed mice, we conducted a comprehensive analysis of various mitochondrial parameters. Compared with the ND group, TBARS levels and H_2O_2 concentrations were significantly elevated in HFD mice, while SOD and ATP content was inhibited; notably, these effects were partially reversed by DMBG (Fig. 3A-D). Measurement of mitochondrial membrane potential suggested that the value of JC-1 aggregation/monomer was decreased in HFD mice, which was reversed by DMBG (Fig. 3E). Moreover, HFD significantly increased mitochondrial ROS intensity and the mtDNA level in mice, which was restored by DMBG (Fig. 3F, G). SIRT5 mRNA level was also reduced in HFD mice, which was elevated by DMBG (Fig. 3H). In addition, western blot results suggested that the protein levels of p-AMPK, PGC-1α and SIRT5 were downregulated in HFD mice, which was partially increased by DMBG (Fig. 3I). In conclusion, we demonstrated that DMBG alleviated the mitochondrial dysfunction in HFD mice.

SIRT5 knockdown inhibits the improvement of mitochondrial function in PA-induced HepG2 cells by DMBG

SIRT5 plays an important role in maintaining energy homeostasis. To further investigate the role of SIRT5 in mitochondrial function and its response to DMBG, we conducted a series of experiments using PA-induced HepG2 cells. Results showed that the expression of SIRT5 was decreased in HepG2 cells with SIRT5 knockdown (Fig. 4A). Then, we found that the glucose consumption was significantly increased in PA-induced cells, which was partially inhibited by DMBG, whereas this inhibition was reversed by SIRT5 knockdown (Fig. 4B). Conversely,

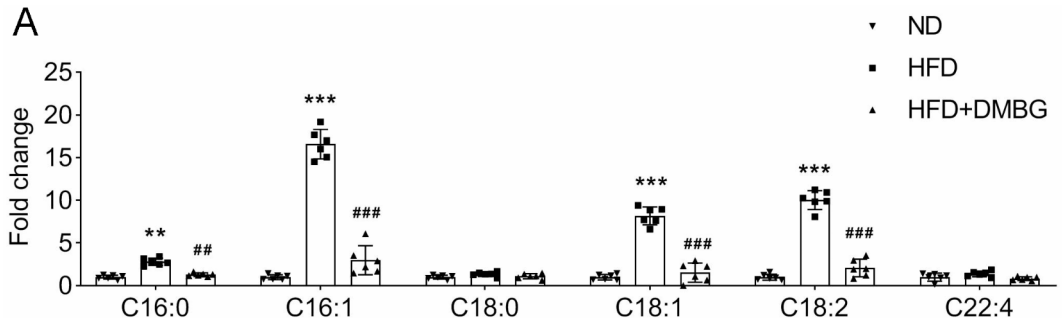

Fig. 1. DMBG inhibited the content FFAs in HFD mice (**A**) The levels of FFAs C16:0, C16:1, C18:0, C18:1, C18:2 and C22:4 in the ND, HFD and HFD + DMBG groups were measured by GC-MS. $^{**}P<0.01$ and $^{***}P<0.001$ vs. the ND group. $\#\#P<0.01$ vs. the HFD group.

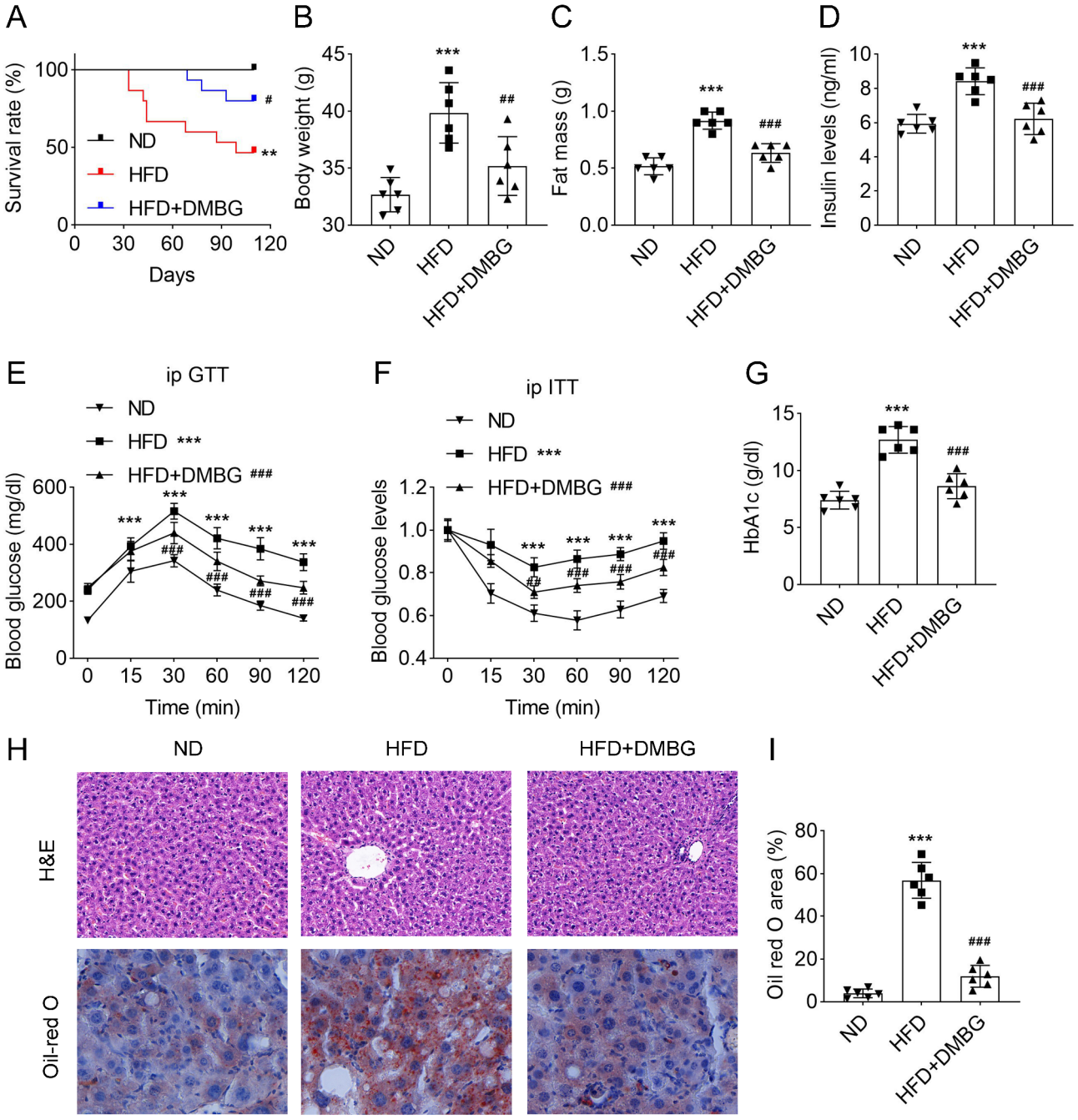

Fig. 2. DMBG inhibited hyperglycemia and liver lipid accumulation in HFD mice (**A**) The survival rate of mice in different groups. (**B-D**) DMBG inhibited the body weight, fat mass and insulin levels increased in HFD mice. (**E** and **F**) The blood glucose levels in the ND, HFD and HFD + DMBG groups were assessed by ip GTT and ip ITT. (**G**) The level of HbA1c increased in HFD mice was reversed by DMBG. (**H**) H&E and Oil red O staining were performed to assess pathological change and lipid accumulation in liver of mice. (**I**) Quantitative results of Oil red O staining. ***$P < 0.001$ vs. The ND group. ##$P < 0.01$ and ###$P < 0.001$ vs. the HFD group.

JC-1 aggregation/monomer levels were reduced in PA-induced HepG2 cells, which was increased by DMBG, and this increase was restored by SIRT5 knockdown (Fig. 4C). The mitochondrial ROS intensity in HepG2 cells was significantly elevated by PA, which was inhibited by DMBG, but the inhibition of mitochondrial ROS intensity was markedly increased by SIRT5 knockdown (Fig. 4D). Additionally, western blot assay showed that the protein levels of p-AMPK, PGC-1α and SIRT5 in HepG2 cells were inhibited by PA, which was upregulated by DMBG, and the increase was inhibited by SIRT5 knockdown (Fig. 4E). In conclusion, these results indicated that SIRT5 knockdown inhibited the improvement of mitochondrial function in PA-induced HepG2 cells by DMBG.

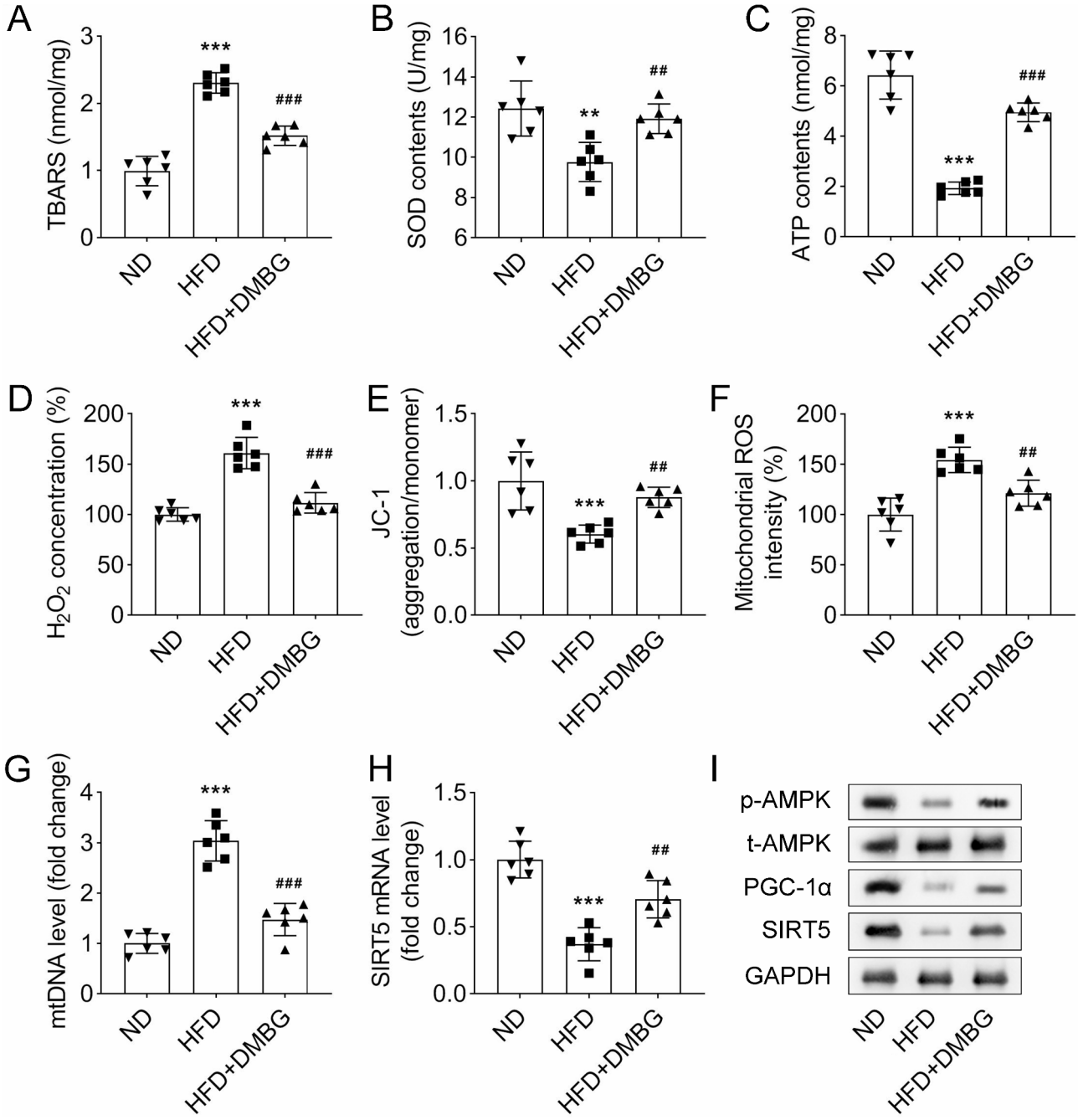

Fig. 3. DMBG alleviated the mitochondrial dysfunction in HFD mice (**A**-**D**) The levels of TBARS, SOD, ATP and H_2O_2 in the liver of mice were measured using a TBARS assay kit, a SOD assay kit, an ATP assay kit and an H_2O_2 assay kit, respectively. (**E**) Mitochondrial membrane potential was presented as polymer/monomer of JC-1. (**F**) Mitochondrial ROS was measured using an ROS assay kit. (**G** and **H**) qPCR was performed to measure the level of mtDNA and SIRT5 expression in different groups. (**I**) The protein levels of p-AMPK, t-AMPK, PGC-1α and SIRT5 was assessed by western blot assay. $^{**}P<0.01$ and $^{***}P<0.001$ vs. the ND group. $\#\#P<0.01$ and $\#\#\#P<0.001$ vs. the HFD group.

SIRT5 mediates the desuccinylation of ECHA at K540 site

Building on previous findings that SIRT5 regulates succinylation on ECHA in the heart of mice[21], we investigated the role of SIRT5 in modulating ECHA succinylation and stability in HepG2 cells. Results showed that overexpression of SIRT5 inhibited ECHA succinylation but upregulated the protein level of ECHA (Fig. 5A). Co-IP revealed the interaction between SIRT5 and ECHA (Fig. 5B). Next, we predicted several succinylation sites and mutate these sites into arginine (R) using point mutation technique to determine which site is modified by succinylation. Results suggested that only K540 mutation increased ECHA succinylation and inhibited the protein level of ECHA in HepG2 cells with SIRT5 overexpression (Fig. 5C). Moreover, we demonstrated that

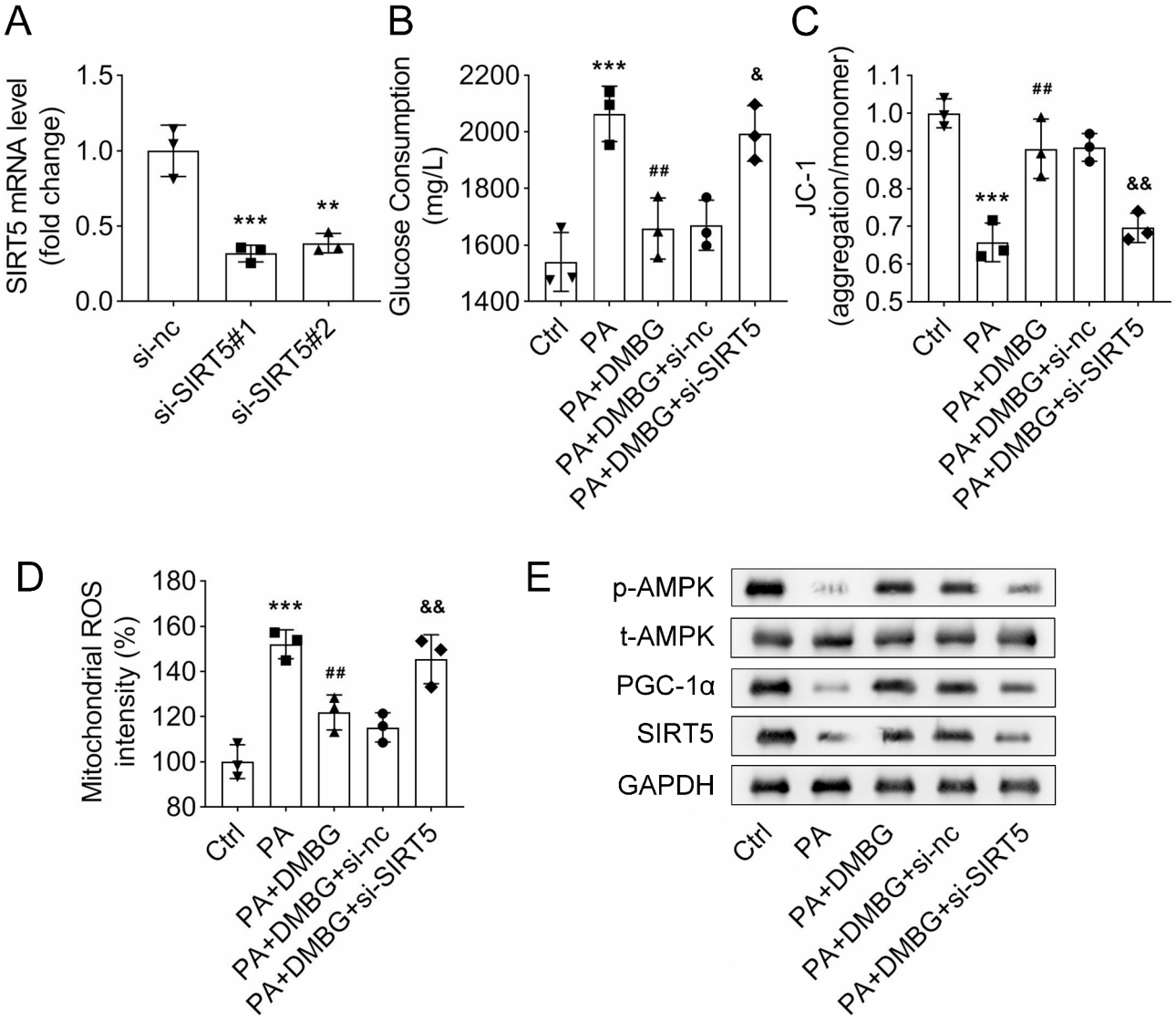

Fig. 4. SIRT5 knockdown inhibits the improvement of mitochondrial function in PA-induced HepG2 cells by DMBG (**A**) The expression of SIRT5 was measured by qPCR. (**B**) The glucose consumption was measured using a Cell Meter 2-NBDG glucose uptake assay kit. (**C**) Mitochondrial membrane potential was presented as polymer/monomer of JC-1. (**D**) Mitochondrial ROS was measured using an ROS assay kit. (**E**) The protein levels of p-AMPK, t-AMPK, PGC-1α and SIRT5 was assessed by western blot assay. ***$P < 0.001$ vs. the si-nc group or the ND group. ##$P < 0.01$ vs. the. PA group. &$P < 0.05$ and &&$P < 0.01$ vs. the PA + DMBG group.

SIRT5 overexpression inhibited the degradation of ECHA, indicating that SIRT5 overexpression increased the protein stability of ECHA (Fig. 5D). These results confirmed that SIRT5 overexpression promoted ECHA desuccinylation at K540 site.

Discussion

Hyperglycemia and abnormal lipid metabolism are hallmark features of T2DM, which, if left uncontrolled, can lead to serious complications such as nephropathy, hypertension, and coronary heart disease. DMBG is a widely prescribed therapeutic agent for T2DM management. Compared to insulin or sulfonylureas, DMBG exhibits minimal side effects, reducing the likelihood of treatment-induced complications[22]. Previous studies have demonstrated that DMBG effectively suppresses hyperglycemia in obese individuals by regulating mitochondrial function. Specifically, it has been shown to enhance mitochondrial respiration, membrane potential, and ATP levels in HFD-fed mice[23]. Horakova et al.[24] observed a 25–50% reduction in blood glucose levels in HFD mice treated with increasing concentrations of DMBG via gavage. Additionally, Hundal et al.[25] reported that DMBG significantly reduced liver gluconeogenesis by more than 33% in human subjects. Beyond its effects on glucose metabolism, DMBG also exerts beneficial influences on lipid homeostasis. For instance, Tehrani et al.[26] found that the combination of DMBG and morin decreased hepatic triglyceride levels and reduced the size and weight of epididymal white adipose tissue (WAT) and subcutaneous WAT in HFD-fed mice. Cheng et al.[27] further

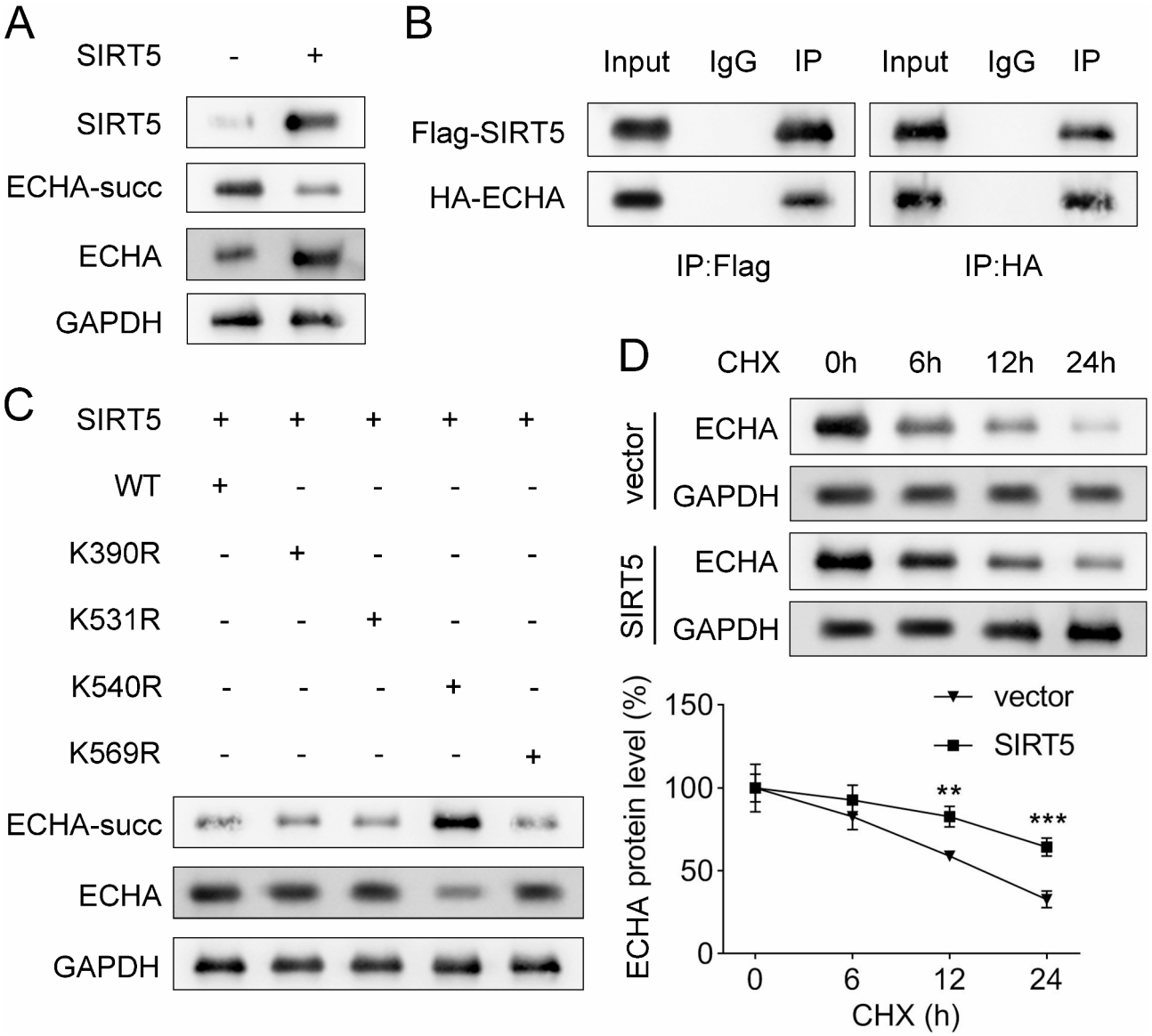

Fig. 5. SIRT5 mediated the desuccinylation of ECHA at K540 site (**A**) Western blot assay was performed to assess SIRT5 protein level as well as the succinylation and protein levels of ECHA. (**B**) The interaction between SIRT5 and ECHA was assessed by co-IP. (**C**) Western blot assay demonstrated that SIRT5 overexpression mediated the desuccinylation of ECHA at K540 site. (**D**) The stability of ECHA protein was assessed using western blot after treatment with 10 μM CHX for 0, 6, 12, and 24 h. $^{**}P < 0.01$ and $^{***}P < 0.001$ vs. the 0 h.

confirmed that DMBG activates the expression of Slc25a47, leading to inhibition of hepatic lipid content, triglycerides, and cholesterol levels in mice. In this study, we provide comprehensive evidence that DMBG mitigates multiple aspects of metabolic dysfunction in HFD-fed mice. Our findings demonstrate that DMBG not only inhibits FFA levels, blood glucose, and insulin but also suppresses liver lipid accumulation and body weight gain. Moreover, DMBG ameliorates mitochondrial dysfunction, thereby improving overall glucolipid metabolism in HFD-fed mice. These results collectively underscore the multifaceted mechanisms through which DMBG exerts its therapeutic effects on metabolic disorders, positioning it as a promising agent for managing T2DM and associated comorbidities.

SIRT5, a mitochondrial desuccinylase, plays a pivotal role in regulating protein succinylation and mitochondrial metabolism. Rardin et al.[28]demonstrated that succinylated proteins are highly enriched in liver mitochondria, and the loss of SIRT5 leads to excessive succinylation of mitochondrial proteins, highlighting its critical function in maintaining mitochondrial homeostasis. SIRT5 has been shown to influence various metabolic pathways. It suppresses the biochemical activities of the pyruvate dehydrogenase complex and succinate dehydrogenase, thereby affecting mitochondrial respiration driven by these complexes[29]. Xiao et al.[30] confirmed that in a subarachnoid hemorrhage mouse model, decreased SIRT5 expression impacts mitochondrial metabolism by inhibiting succinylated citrate synthase and ATP synthase subunits, leading to reduced ATP production and

increased ROS generation. Recent studies have also implicated SIRT5 in glucose metabolism. Wang et al.[31] found that the absence of SIRT5 in brown adipose tissue impairs the transition from free fatty acids to glucose. Zhang et al.[32] reported that LPS treatment in SIRT5-deficient mice resulted in lower blood glucose levels and higher insulin levels, suggesting a role for SIRT5 in glucose homeostasis. Ou et al.[33] observed that SIRT5 knockdown in mesenchymal stem cells reduced ROS accumulation and increased glucose uptake, further emphasizing its involvement in metabolic regulation. In our study, we found that SIRT5 expression was downregulated in HFD-fed mice but was restored by DMBG treatment through the activation of AMPK. This finding aligns with previous observations by Buler et al.[18],reinforcing the notion that DMBG can modulate SIRT5 expression via AMPK signaling. Moreover, DMBG inhibited glucose consumption and improved mitochondrial dysfunction in palmitic acid (PA)-induced HepG2 cells, effects that were reversed upon SIRT5 knockdown. These results collectively demonstrate that DMBG ameliorates hyperglycemia and mitochondrial dysfunction by enhancing SIRT5 expression.

ECHA is a critical enzyme in mitochondrial fatty acid oxidation, playing an essential role in energy metabolism. Overexpression of ECHA has been shown to reduce insulin release, thereby influencing glucose levels[34]. Pan et al.[19] demonstrated that ECHA acts as a negative regulator of hepatic gluconeogenesis; its downstream metabolite β-hydroxybutyrate maintains FOXO1 acetylation, which inhibits ECHA-mediated hepatic gluconeogenesis. Ding et al.[20] confirmed that elevated ECHA levels decrease lipid accumulation and steatosis in the mouse liver. Collectively, these findings highlight the involvement of ECHA in the regulation of glucolipid metabolism. Additionally, Sadhukhan et al.[21] revealed that SIRT5 activates ECHA through deacetylation, modulating cardiac fatty acid metabolism and ATP production. However, the extent to which ECHA deacetylation influences glucose and lipid metabolism remains an open question. In this study, we provide novel insights into the regulatory mechanisms involving SIRT5 and ECHA. Specifically, our results demonstrate that overexpression of SIRT5 promotes desuccinylation of ECHA at the K540 site. This post-translational modification not only alters the functional state of ECHA but also enhances its protein stability, leading to increased ECHA protein levels. The identification of K540 as a specific succinylation site regulated by SIRT5 underscores the intricate interplay between post-translational modifications and metabolic enzyme function.

In conclusion, our study definitively demonstrates that DMBG ameliorated hepatic glucose and lipid metabolic disorders as well as mitochondrial dysfunction in HFD-fed mice through SIRT5-mediated desuccinylation of ECHA. These findings suggest a promising therapeutic target for addressing hyperglycemia and lipid metabolism abnormalities in T2DM.

Data availability

The datasets used and/or analyzed during the current study are available from the corresponding author on reasonable request.

Received: 13 November 2024; Accepted: 3 March 2025
Published online: 05 March 2025

References

1. Demir, S., Nawroth, P. P., Herzig, S. & Ekim Üstünel, B. Emerging targets in type 2 diabetes and diabetic complications. *ADV. SCI.* **8**, e2100275 (2021).
2. Ruze, R. et al. Obesity and type 2 diabetes mellitus: connections in epidemiology, pathogenesis, and treatments. *Front. Endocrinol. (Lausanne).* **14**, 1161521 (2023).
3. He, F. et al. Mitophagy-mediated adipose inflammation contributes to type 2 diabetes with hepatic insulin resistance. *J. Exp. Med.* **218**, (2021).
4. Wang, Y. et al. Ameliorates inflammation and lipid metabolism by regulating macrophage polarization and mitochondrial dynamics in the liver of type 2 diabetes mellitus mice. *Metabolites* **13**, 14 (2022).
5. Lanthier, N. et al. Kupffer cell activation is a causal factor for hepatic insulin resistance. *Am. J. Physiol. Gastrointest. Liver Physiol.* **298**, G107 (2010).
6. Pinti, M. V. et al. Mitochondrial dysfunction in type 2 diabetes mellitus: an organ-based analysis. *Am. J. Physiology: Endocrinol. Metabolism.* **316**, E268 (2019).
7. Rena, G., Hardie, D. G. & Pearson, E. R. The mechanisms of action of Metformin. *DIABETOLOGIA* **60**, 1577 (2017).
8. LaMoia, T. E. & Shulman, G. I. Cellular and molecular mechanisms of Metformin action. *ENDOCR. REV.* **42**, 77 (2021).
9. Petrie, J. R. et al. Cardiovascular and metabolic effects of Metformin in patients with type 1 diabetes (REMOVAL): a double-blind, randomised, placebo-controlled trial. *Lancet Diabetes Endocrinol.* **5**, 597 (2017).
10. Liu, H. et al. Metformin suppresses calcium oxalate crystal-induced kidney injury by promoting Sirt1 and M2 macrophage-mediated anti-inflammatory activation. *Signal. Transduct. Target. Ther.* **8**, 38 (2023).
11. Yang, J. et al. Metformin induces ferroptosis by inhibiting ufmylation of SLC7A11 in breast cancer. *J. Exp. Clin. Cancer Res.* **40**, 206 (2021).
12. Du, M. R. et al. Exploring the Pharmacological potential of Metformin for neurodegenerative diseases. *FRONT. AGING NEUROSCI.* **14**, 838173 (2022).
13. Xie, Z. et al. Lysine succinylation and lysine malonylation in histones. *MOL. CELL. Proteom.* **11**, 100 (2012).
14. Du, J. et al. Sirt5 is a NAD-dependent protein lysine demalonylase and desuccinylase. *SCIENCE* **334**, 806 (2011).
15. Fabbrizi, E. et al. Emerging Roles of SIRT5 in Metabolism, Cancer, and SARS-CoV-2 Infection. *CELLS-BASEL* **12**, (2023).
16. Hu, T. et al. Metabolic Rewiring by Loss of Sirt5 Promotes Kras-Induced Pancreatic Cancer Progression. *GASTROENTEROLOGY* **161**, 1584 (2021).
17. Song, J. et al. Distinctive roles of sirtuins on diabetes, protective or detrimental?? *Front. Endocrinol. (Lausanne).* **9**, 724 (2018).
18. Buler, M., Aatsinki, S. M., Izzi, V., Uusimaa, J. & Hakkola, J. SIRT5 is under the control of PGC-1alpha and AMPK and is involved in regulation of mitochondrial energy metabolism. *FASEB J.* **28**, 3225 (2014).
19. Pan, A. et al. The mitochondrial beta-oxidation enzyme HADHA restrains hepatic glucagon response by promoting beta-hydroxybutyrate production. *NAT. COMMUN.* **13**, 386 (2022).
20. Ding, J. et al. HADHA alleviates hepatic steatosis and oxidative stress in NAFLD via inactivation of the MKK3/MAPK pathway. *MOL. BIOL. REP.* **50**, 961 (2023).

21. Sadhukhan, S. et al. Metabolomics-assisted proteomics identifies succinylation and SIRT5 as important regulators of cardiac function. *Proceedings of the National Academy of Sciences - PNAS* **113**, 4320 (2016).
22. Taylor, S. I., Yazdi, Z. S. & Beitelshees, A. L. Pharmacological treatment of hyperglycemia in type 2 diabetes. *J. CLIN. INVEST.* **131**, (2021).
23. Wang, Y. et al. Metformin improves mitochondrial respiratory activity through activation of AMPK. *Cell. Rep. (Cambridge).* **29**, 1511 (2019).
24. Horakova, O. et al. Metformin acutely lowers blood glucose levels by Inhibition of intestinal glucose transport. *Sci. Rep.* **9**, 6156 (2019).
25. HUNDAL, R. S. et al. Mechanism by which metformin reduces glucose production in type 2 diabetes. *Diabetes (New York, N.Y.)* **49**, 2063 (2000).
26. Tehrani, S. S., Goodarzi, G., Panahi, G., Zamani-Garmsiri, F. & Meshkani, R. The combination of metformin with morin alleviates hepatic steatosis via modulating hepatic lipid metabolism, hepatic inflammation, brown adipose tissue thermogenesis, and white adipose tissue browning in high-fat diet-fed mice. *Life sciences (1973)* **323**, 121706 (2023).
27. Cheng, L. et al. Hepatic mitochondrial NAD + transporter SLC25A47 activates AMPKα mediating lipid metabolism and tumorigenesis. *Hepatol. (Baltimore Md).* **78**, 1828 (2023).
28. Rardin, M. J. et al. SIRT5 regulates the mitochondrial lysine succinylome and metabolic networks. *CELL. METAB.* **18**, 920 (2013).
29. Park, J. et al. SIRT5-mediated lysine desuccinylation impacts diverse metabolic pathways. *MOL. CELL.* **50**, 919 (2013).
30. Xiao, Z. et al. Sirtuin 5-Mediated lysine desuccinylation protects mitochondrial metabolism following subarachnoid hemorrhage in mice. *Stroke (1970).* **52**, 4043 (2021).
31. Wang, G. et al. Regulation of UCP1 and mitochondrial metabolism in brown adipose tissue by reversible succinylation. *MOL. CELL.* **74**, 844 (2019).
32. Zhang, C. et al. SIRT5 is important for bacterial infection by regulating insulin secretion and glucose homeostasis. *PROTEIN CELL.* **11**, 846 (2020).
33. Ou, T. et al. SIRT5 deficiency enhances the proliferative and therapeutic capacities of adipose-derived mesenchymal stem cells via metabolic switching. *Clin. Transl Med.* **10**, e172 (2020).
34. Zhang, Y. et al. The pivotal role. Of protein acetylation in linking glucose and fatty acid metabolism to β-cell function. *Cell. Death. Dis.* **10**, 66 (2019).

Author contributions
SP conceived the study; LT conducted the experiments; QS and JL analyzed the data; LT was a major contributor in writing the manuscript. All authors read and approved the final manuscript.

Funding
This study was supported by Fuling District Science and Technology Commission (FLKJ, 2022AAN1014).

Declarations

Ethics approval and consent to participate
The study was approved by the Ethics Committee of MDKN Biotechnology Co., Lt. All experiments were performed in accordance with relevant guidelines and regulations. This study is reported in accordance with ARRIVE guidelines.

Consent for publication
All authors approved the final manuscript and the submission to this journal.

Competing interests
The authors declare no competing interests.

Additional information
Supplementary Information The online version contains supplementary material available at https://doi.org/10.1038/s41598-025-92716-z.

Correspondence and requests for materials should be addressed to S.P.

Reprints and permissions information is available at www.nature.com/reprints.

Publisher's note Springer Nature remains neutral with regard to jurisdictional claims in published maps and institutional affiliations.